Numerical based design of protection systems against landslides

Francesca Ceccato, Paolo Simonini

Abstract: Fast flow-like landslides are one of the most dangerous natural hazards. Rigid or flexible structures are often used to stop, deviate or slow down the flow. Because of the complexity of the landslide-barrier interaction, the design of these defence structures is still based on oversimplified empirical approaches. Numerical methods able to capture the essential features of the phenomenon can offer a valuable tool to gain a better understanding of the impact process and to support the design of protection measures. This paper shows the potentialities of the Material Point Method (MPM) in this field. The run-up of the landslide and the dynamic forces on the structure are some of the fundamental parameters to define the properties of the barrier which are considered in this paper.

1 Introduction

Landslides of the flow-type, such as debris avalanches, debris flows, and rock avalanches, are among the most dangerous natural hazards. To reduce the risk, different mitigation measures can be applied: active measures include, for example, the stabilization of a potential landslide prior to mobilization; passive measures are, for example, the construction of defence structures in order to stop, deviate or slow down the flow. In many cases active measures are unfeasible, thus the design of a system of protection barriers is necessary. A common type of protective structure is a dyke or wall placed at the boundary of a storage basin, which will accommodate the volume of incoming material, see e.g. Figure 1. These structures are designed to stop the motion of the landslide before reaching the protected area and they are also called *terminal barriers*.

Important quantitative parameters for the design of terminal barriers are the run-up of a potential landslide against the face of the structure (the dyke crest must be sufficiently high to avoid overtopping), and the forces exerted by the moving debris on the face of the structure.

These parameters are often estimated with simplified, empirically based relationships, such as those proposed by Harbitz et al. (2000), but numerical modelling of landslide motion can provide a fundamental support for the design of protective structures.

The majority of existing models simulating the motion of landslides and avalanches are based on depth-averaged techniques that adapt existing hydraulics theory to the flow of granular (frictional) materials (Savage 1998; Pastor et al. 2009). This approach demonstrated to be successful in predicting the movement of frictional flows over complex topologies; however, because of

the averaging of quantities along depth, it is inappropriate to estimate the impact forces on the structures.

More appropriate numerical techniques for the study of impact forces are Eulerian methods (Moriguchi et al. 2009), discrete element methods (Leonardi et al. 2014; Calvetti et al. 2016) and Lagrangian particle-based methods such as SPH, PFEM, FEMLIP, MPM (Idelsohn et al. 2006; Bui and Fukagawa 2013; Mast et al. 2014a; Prime et al. 2014; Ceccato 2016). The latter is considered particularly promising and its potentialities are explored in this paper.

The Material Point Method (MPM) has been specifically developed for large deformations of history dependent materials. It simulates large displacements by Lagrangian points moving through an Eulerian grid as shortly described in Section 2.

Numerical modelling of landslide-structure interaction is challenging because the process involves large deformations, contact issues and complex thermo-hydro-mechanical processes that have not been fully understood yet. In this paper, we consider a single-phase material, whose mechanical response is modelled with a linear elastic perfectly plastic constitutive law with Mohr-Coulomb failure criterion. In reality, the behaviour of granular flows is more complex, and it will be further investigated in future developments of the research. The use of the Mohr-Coulomb model is considered appropriate in this stage of the research; moreover, it has been observed that the Coulomb friction generates most of the stress in dense granular flows (Iverson 1997).

A 3D MPM code, named *Anura3D*, featuring a specific algorithm to model soil-structure interaction is here applied to the study of the run-up of rapid landslides against a terminal barrier and the impact forces on a dam.

The simulation of landslide run-up considers a set of experimental results, published in Mancarella and Hungr (2010), where a mass of dry sand is instantly released at the top of a channel, it flows down and it is arrested by a steep adverse slope. The results of the numerical simulations are presented in Section 3.2 where a good agreement with the experimental evidences can be appreciated.

The impact forces on a rigid structure are investigated placing the soil mass in front of the barrier with an initial prescribed velocity, thus the propagation phase of the landslide is disregarded in this study. This work investigated the effect of the shape of the flow front and the inclination of the barrier face. In Section 4 the results of these simulation are presented, highlighting how the numerical model can be useful for an effective design of these structures.

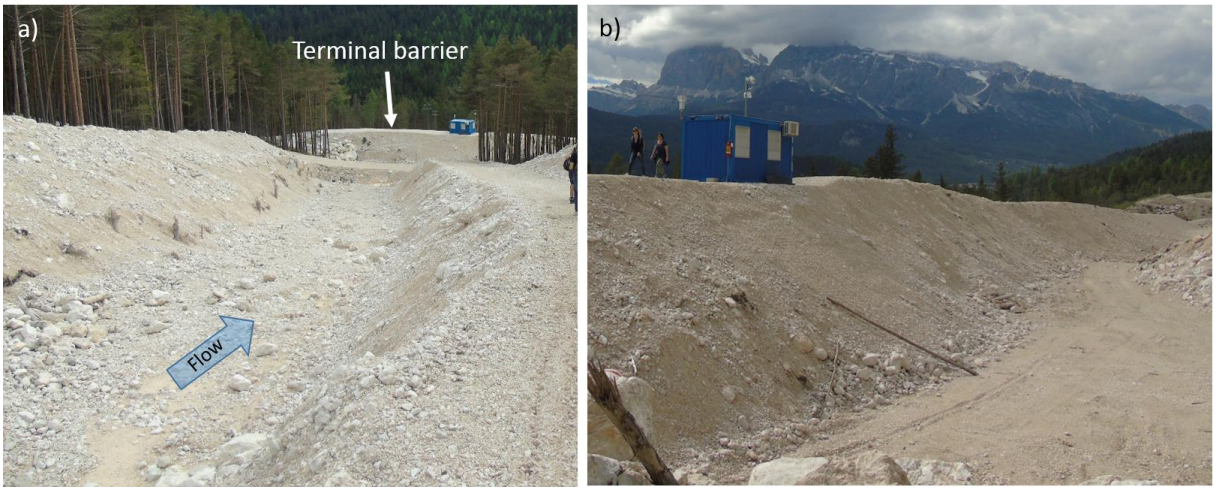

Figure 1 Example of protection barrier against debris flow in Cortina d'Ampezzo (Italy) (a) view of the channel and terminal barrier; (b) view of the barrier

2 The Material Point Method: basic concepts

MPM is a particle-based method developed since the 90's for large deformations of history dependent materials (Sulsky et al. 1994). Recently, the method has been extended to coupled problems in order to simulate the soil-water interaction in saturated soils (Abe et al. 2013; Jassim et al. 2013; Martinelli and Rohe 2015) and unsaturated conditions (Yerro et al. 2015). MPM has been successfully applied to the simulation of a number of geotechnical problems such as slope stability (Andersen and Andersen 2010), collapse of dams (Alonso and Zabala 2011) and river-banks (Bandara and Soga 2015), cone penetration (Beuth and Vermeer 2013; Ceccato et al. 2015; Ceccato and Simonini 2016), and impact of granular avalanches on rigid obstacles (Mast et al. 2014b; Ceccato 2016).

The continuum body is discretized by a set of Lagrangian points, called material points (MP). They carry all the information of the continuum such as density, velocity, acceleration, stress, strain, material parameter as well as external loads. The MP do not represent single soil grains, as in DEM, but a portion of the continuum body. Large deformations are simulated by MP moving through a fixed computational finite element mesh, which covers the entire region of space into which the solid is expected to move. This grid is used to solve the system of equilibrium equations, but does not deform with the body like in Lagrangian Finite Element Method.

At the beginning of each time increment, the information is mapped from the MP to the computational nodes of the mesh by means of the interpolation functions (Fig. 1a). The governing equations of motion are solved (Fig. 1b) and the nodal values are used to update the velocity, the position and to compute strains and stresses at the MP (Fig. 1c). At the end of the time step, the mesh may be changed arbitrarily, but it is usually kept fix. The assignment of MP to finite elements is updated after mesh adjustment (Fig. 1d).

The applied software, *Anura3D*, is currently under development by a research community including Deltares (The Netherlands), University of Cambridge (UK), University of Catalunya (Barcelona, Spain), TU Hamburg–Harburg (Germany), University of Padua (Italy), TU Delft (The Netherlands) and University of California Berkeley (USA). It implements an enhanced version of the original MPM, which has been extensively validated for geomechanical problems (Ceccato et al. 2016; Fern et al. 2016; Phuong et al. 2016; Bolognin et al. 2017).

The software applies 4-noded linear tetrahedral elements. Problems of volumetric locking, typically affecting low-order elements, are mitigated by the use of an "enhanced strain" based on the Nodal mixed Discretization technique proposed by Detournay and Dzik (2006).

The frictional contact is modelled by the multi-velocity field contact algorithm proposed by Bardenhagen et al. (2001) as implemented in the software *Anura3D* (Al-Kafaji 2013; Ceccato et al. 2016; Ceccato et al. 2017). In this approach, the contact is solved at the nodal level: the velocities at the nodes of the contact surface are predicted from the solution of each body separately and then corrected imposing the impenetrability condition and the Coulomb's friction criterion.

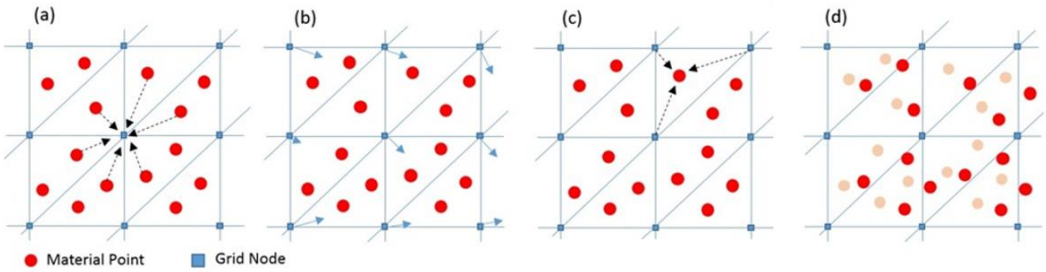

Figure 2 Computation scheme of MPM: a) map information to the nodes, (b) solve the governing equations of motions at the nodes, (c) update MP quantities (d) update MP housekeeping

3 Study of landslide run-up on terminal barriers

In this section we consider the experimental experience by Mancarella and Hungr (2010). A volume of 0.027 m^3 of dry sand was placed in a reservoir of triangular cross section placed at the top of a 29°-steep channel. The granular material was released instantly and it flows down reaching the bottom of the slope and then runs up an adverse ramp.
The effect of the inclination of the run-up slope on the run-up height is investigated. The run-up height is defined as the vertical distance between the lowest point of the channel and the highest level reached by the flow on the run-up slope. The velocity and the position of the flow front where also monitored.

3.1 Geometry, discretization and material parameters

The geometry and the material parameters applied in the numerical model follow strictly the experiment specifications (see Figure 3 and Table 1). No tuning of the parameters is performed to fit the laboratory results. However, since the problem is essentially bi-dimensional, the width of the model is only 0.02m instead of 0.35m. The transition radius at the lowest point of the model is 0.10m. We consider an inclination of the run-up slope equal to 7°, 33° and 61° to the horizontal.
The discretization is determined through preliminary analyses as a compromise between accuracy and computational costs. A fine mesh is used at the sliding base to ensure a more accurate application of the contact algorithm. 20 MP are placed inside each element of the volume defining the initial position of the soil. 4 MP per element are used for the channel base which is kept fix in space.
Roller boundary conditions are prescribed at the lateral surfaces and the base of the model is fully fixed.

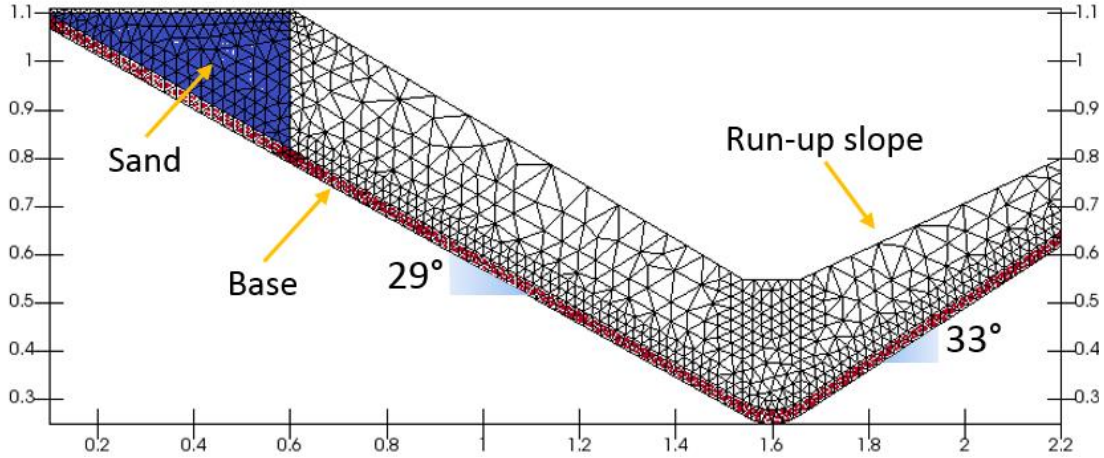

Figure 3 Geometry and discretization of the MPM model for an inclination of the run-up slope of 33° (5307 linear tetrahedral elements, 10884 nodes, 15430 MP)

Table 1 material constitutive parameters

Parameter	Symbol	Value
Solid density [kg/m^3]	ρ_s	2673
Porosity [-]	n	0.39
Friction angle [°]	φ	30.9
Young modulus [kPa]	E	500
Poisson ratio [-]	ν	0.2
Basal friction coefficient [-]	μ	0.40

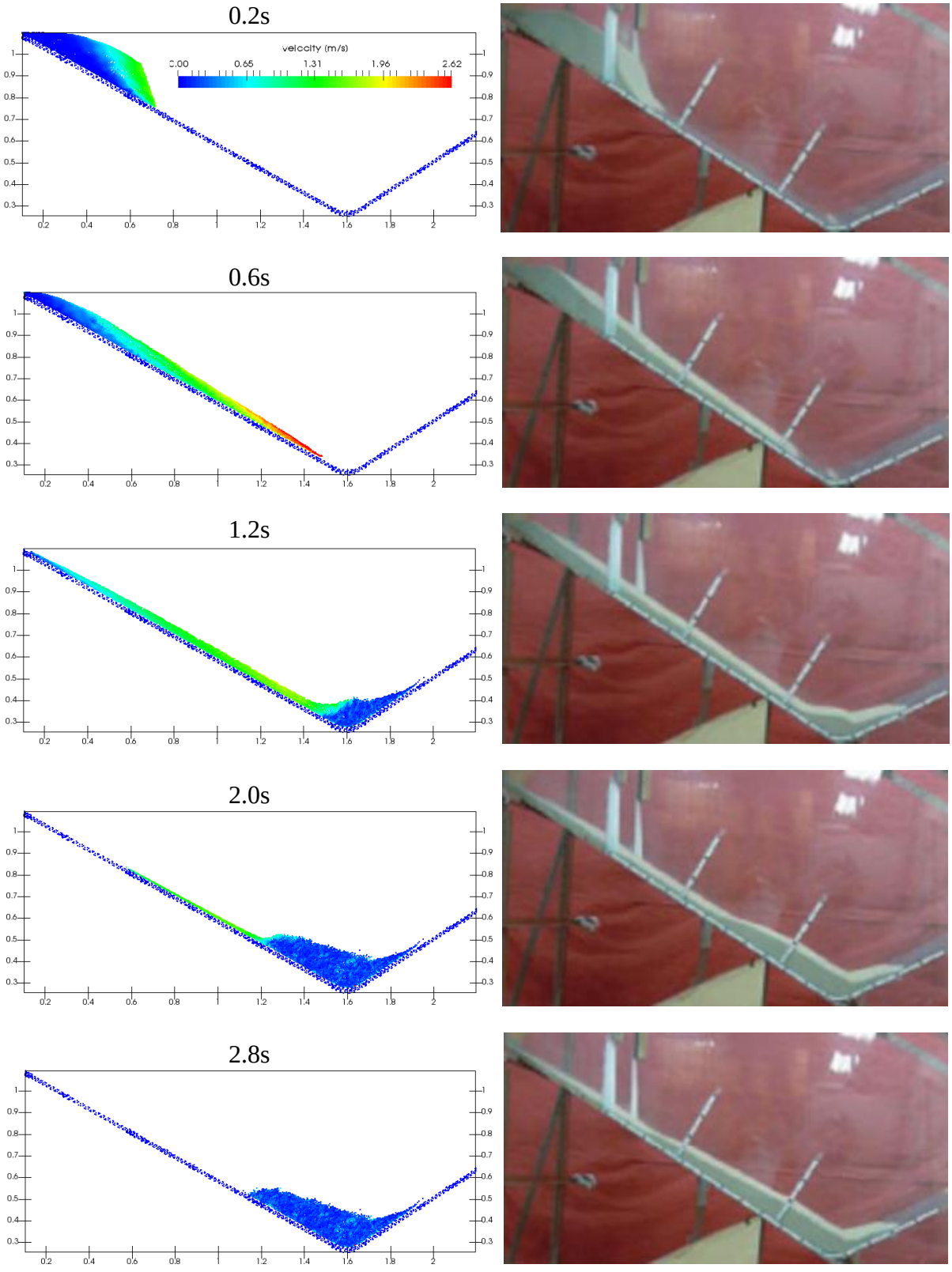

Figure 4 Development of the sand motion and comparison with the experiments by Mancarella and Hungr (2010) (after Ceccato 2017)

3.2 Results

We first consider an inclination of the run-up slope of 33°.The evolution of the flow profile predicted with the numerical simulation is compared with the experimental results in Figure 4. There is a very good agreement up to the maximum run-up (1.2s), which is only slightly higher than the experimental one, but the final shape of the deposit differs from the experiment. In particular, the length of the deposit is smaller in the simulation. This may be due to the constitutive model, which does not fully capture the behaviour of the granular flow.
Figure 5 and Figure 6 plot the displacement and velocity of the flow front respectively. In MPM, a few MP tend to separate from the rest of the flow, and they move ahead faster, but the flow position and velocity is not identified with these MP; in contrast, an average of the first 20 MP is considered. The numerical and the experimental results compares well. The velocity of the front is maximum when it reaches the curvature at the base of the slope, this value of velocity is considered as a reference and named *impact velocity*.
We also considered a front inclination of 7° and 61°. The shape of the landslide at the maximum run-up and of the final deposit are shown in Figure 7. The flow profile at the maximum run-up is well captured although there are a few isolated MP that move ahead determining an overestimation of the run-up height.
Further details on the MPM simulation of this problem and the results of parametric analyses can be found in Ceccato (2017).

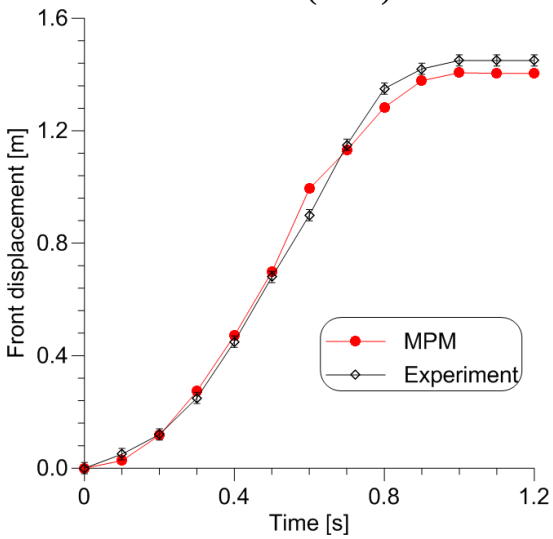

Figure 5 Displacement of the flow front with time (Ceccato 2017)

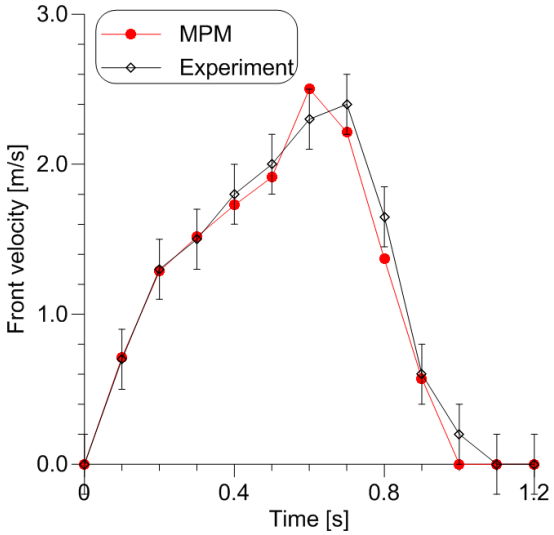

Figure 6 Velocity of the flow front with time (Ceccato 2017)

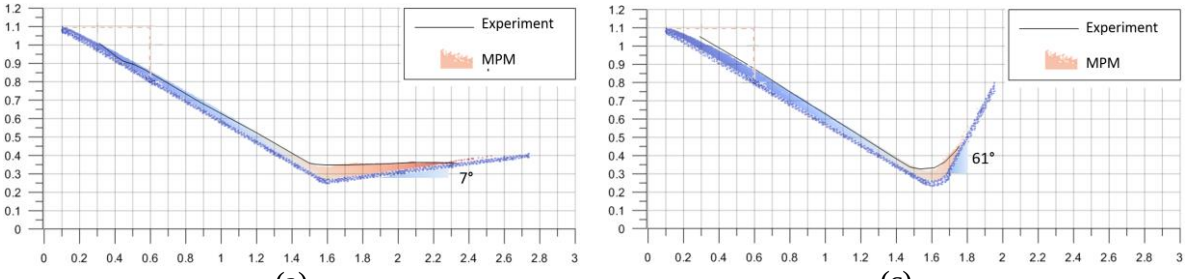

(a) (c)

Figure 7 Comparison between numerical and experimental profile at the maximum run-up for an inclination of the ramp of 7° (a) and 61° (b) (Ceccato 2017)

4 Study of impact forces on rigid barriers

In this Section we analyse in details the phenomenon of impact against a rigid barrier. We do not consider the flow propagation like in the previous section, but we focus on the first seconds of the impact. The mass is initially positioned in front of the barrier with a prescribed velocity v_0 (Figure 8).
The flow is 3.0m thick and 15.0m long. The model is 0.2m wide. The numerical results are normalized with respect to the model width. The obstacle is 6m-high and all the boundaries are assumed to be smooth. Different inclinations of the front (α) and different inclinations of the barrier face (β) are considered. The structure is assumed to be rigid, i.e. the MP do not move and the nodal velocity is zero.
The mesh is refined in the proximity of the obstacle. 20 MPs are initially placed inside each active element (yellow colour in Figure 8).
The behaviour of the soil is modelled with a linear elastic perfectly plastic model with Mohr-Coulomb failure criterion. The reference parameters are summarized in Table 2.

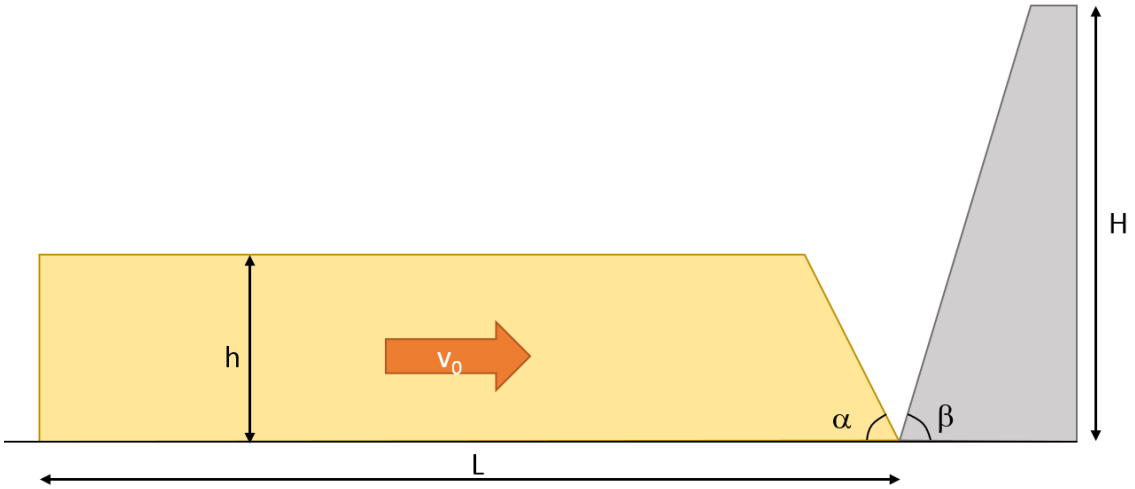

Figure 8 Geometry of the model for the study of landslide impact

Table 2 Material constitutive parameters

Parameter	Symbol	Value
Solid density [kg/m^3]	ρ_s	2650
Porosity [-]	n	0.45
Friction angle [°]	φ	33
Young modulus [kPa]	E	58000
Poisson ratio [-]	ν	0.2

4.1 Description of the impact process

In this section we discuss the essential features of the impact process by considering a landslide hitting a vertical barrier with a velocity of 8.8m/s and a front parallel to the wall face, i.e. α=90°, β=90°, v_0=8.8m/s.
When the granular flow hits the obstacle, it suddenly decelerates and compacts against the wall. This generates a compression shock wave that propagates upstream with a celerity that is close to the sound speed, see Figure 9. The stress behind this shock determines the force on the obstacle at the instant of the impact.

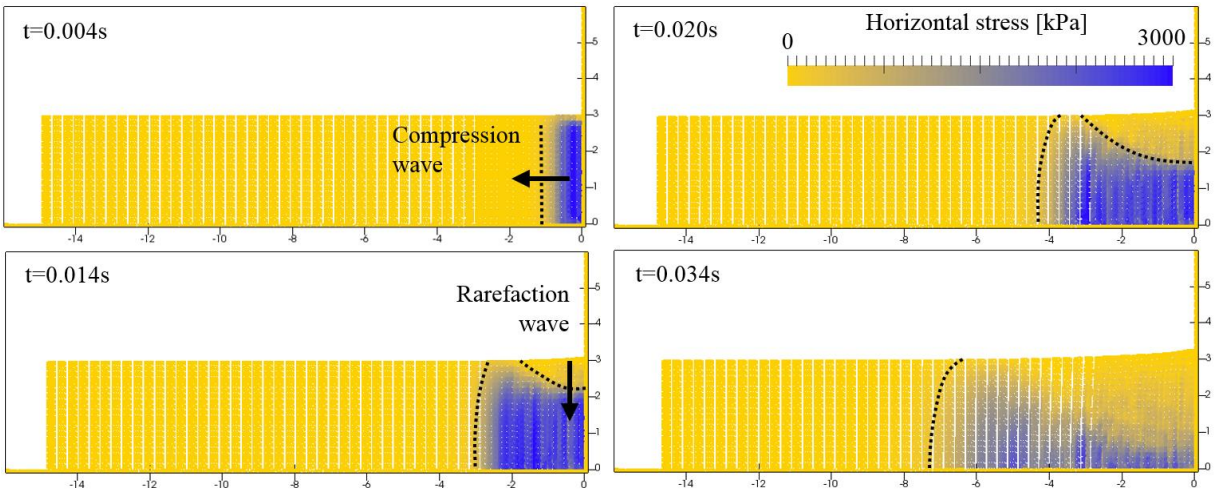

Figure 9 Horizontal stress contour at different time (α=90°, β=90°, v_0=8.8m/s)

This phenomenon is the well-known water hammer phenomenon studied in hydraulics. In case of confined flow, i.e. absence of open boundaries, this high pressure remains constant for a relatively long time. In contrast, in a free-surface granular flow, the lack of confinement generates a rarefaction wave, causing a progressive decrease of the effective stress.
Because of this interaction with the free surface, the impact force reaches a peak and rapidly decreases as shown in Figure 10. Increasing the impact velocity, the maximum impact force increases proportionally.
We can define a dynamic increment of horizontal stress as

$$\Delta\sigma'_{dyn} = \sigma'_x - \sigma'_{x0}$$

where σ'_{x0} =litostatic initial horizontal stress. At the time of maximum impact force (peak time, t_{peak}), $\Delta\sigma'_{dyn}$ has a constant distribution along the wall height, except in the vicinity of the flow boundary, where it rapidly decreases (Figure 11). The horizontal stress on the wall progressively decreases with time starting from the top boundary; the rectangular distribution is lost and the arm of the resultant force with respect to the barrier base decreases (Figure 11).

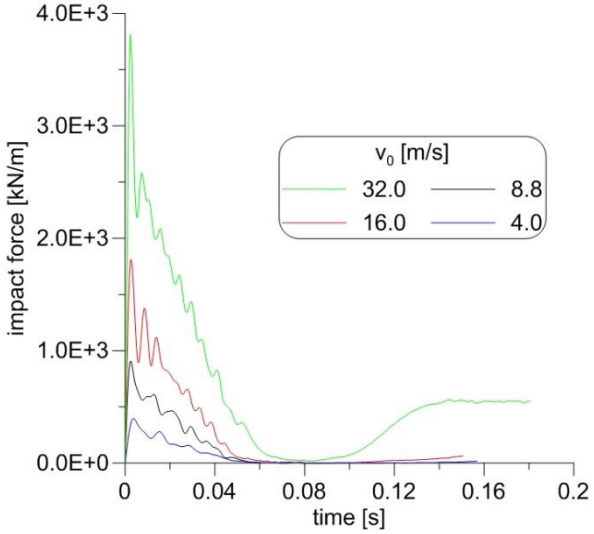

Figure 10 Force on the wall for different impact velocities (α=90°, β=90°)

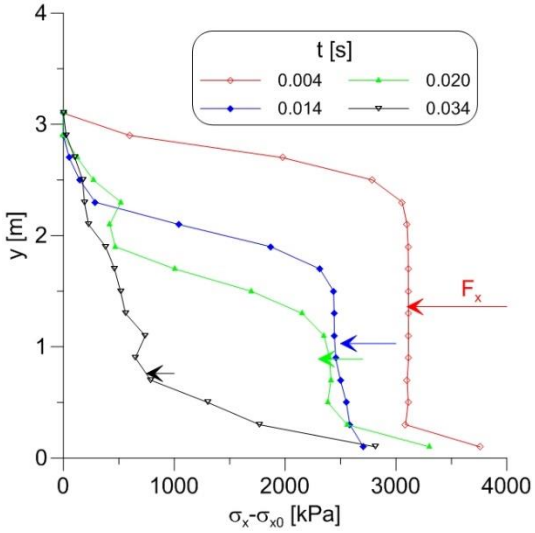

Figure 11 distribution of the dynamic increment of horizontal stress along the wall at different time (α=90°, β=90°, v_0=8.8m/s)

4.2 Effect of front inclination

The effect of the front shape on the force evolution has rarely been taken into account, because it is experimentally difficult to consider and almost impossible to evaluate in real cases. To the authors' knowledge, this aspect has been critically considered only in Calvetti et al. (2016), by discussing DEM numerical results.

When a granular mass flows along a natural slope, the inclination of the front is related to numerous factors such as the slope inclination, the coefficient of lateral soil mass spreading, the average velocity of the sliding mass, the overall friction angle and the density of the soil mass (Ishikawa et al. 2008; Leonardi et al. 2015; Saingier et al. 2016). These aspects are not investigated in the following, but we will discuss the effect of the front inclination in the impact force evolution.

In Section 4.1, we saw that the interaction between the compression waves and the free boundaries of the landslide generates rarefaction waves that modify the stress distribution along the wall and the total impact force. When the flow front is not parallel to the wall face, this effect is even more significant, as shown in Figure 12; moreover, the shape of the free boundary changes with time.

This geometrical effect modifies the evolution of the impact force: decreasing the front inclination, the peak force decreases and the peak time increases (Figure 13). Indeed, the force on the structure depends on both the horizontal stress and the thickness of the material in contact with the wall. The stress is determined by generation and reflection of compression waves at the boundary; it changes with time and elevation, but in general it decreases with α. The thickness of material in contact with the wall increases with time as function of α and v_0.

In case of α=90° the peak force increases linearly with the impact velocity, but for different front inclinations this linear trend is no longer valid (Figure 14).

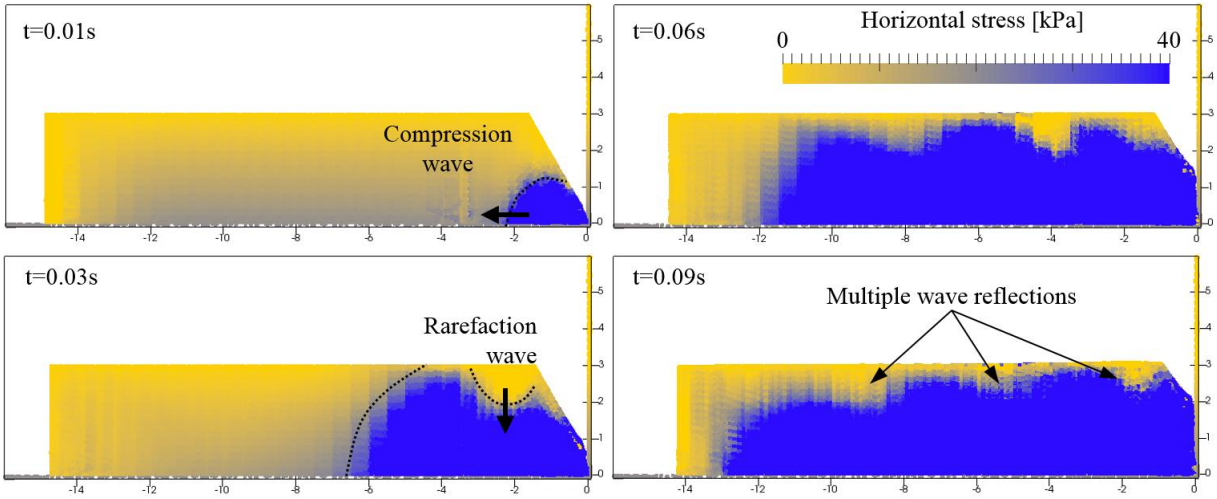

Figure 12 Horizontal stress contour at different time (α=60°, β=90°, v_0=8.8m/s)

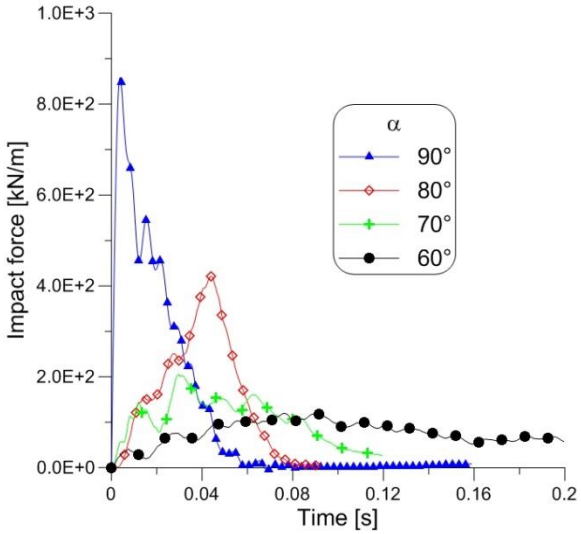

Figure 13 Force evolution for different front inclinations (β=90°, v_0=8.8m/s)

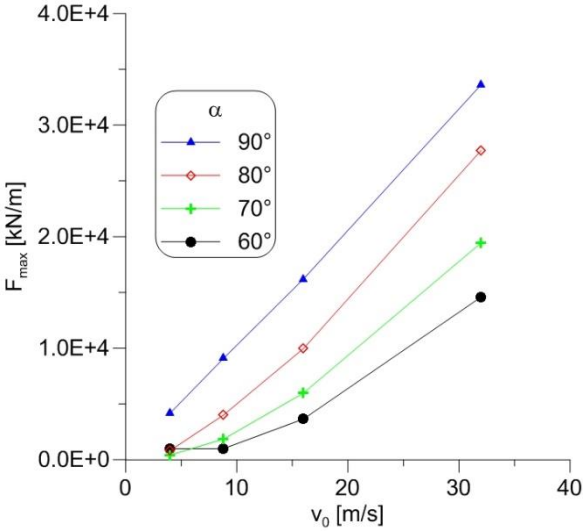

Figure 14 Maximum impact force for different impact velocities and front inclinations (β=90°)

4.3 Effect of barrier inclination

In many cases, defence structures consist in an embankment with a slanted face. The material climbs the wall decelerating and it exerts a pressure on the surface, which has a horizontal and a vertical component. In order to design the structure, both these components are important and they are considered separately in the following. In this Section, the contact between the dam and the soil is smooth; different properties of the interface are considered in Section 4.4.

Slanted structures can be built with compacted granular materials or with the use of geosynthetics to improve soil strengths and reduce the dimensions of the dam by using steeper faces. An important parameter for the design of the geogrids applied in earth reinforced walls (ERW) is the horizontal force at the level of a potential sliding plane between the soil and the geogrid. Moreover, the global stability of the dam must be considered. Several procedures have been proposed for the design of these structures in static conditions (Berg et al. 2009; Berg et al. 2009), but their design under impact loading is not yet supported by a comprehensive scientific literature. Numerical simulations are a valuable tool for an efficient design of these structures.

The impact force components (F_x, F_y) increase with time and reach a peak at a time which is not coincident for the two components, but the two instants are very close (Figure 15). Decreasing the structure face inclination β, the horizontal force decreases, while the reduction of maximum vertical force is less important. The horizontal force is significantly lower than the case of β=90°, moreover F_{max} varies non-linearly with v_0 (Figure 16).

We can divide the wall in a desired number of horizontal slices, 8 in this case, and investigate the evolution of the force applied in each strip as shown in Figure 17. This may be of interest for the definition of the length of the reinforcements in ERW.

The reinforcements that are closer to the base of the wall experiences the highest impact forces (strip number 1 in Figure 17). The impact force reaches its maximum at a different time for each considered strip, thus the pressure distribution assumed for the global stability of the structure could be inaccurate to study the internal stability of the wall. The maximum impact forces for each strip is shown in Figure 18 where it should be noted that the maximum force increases non-linearly with depth.

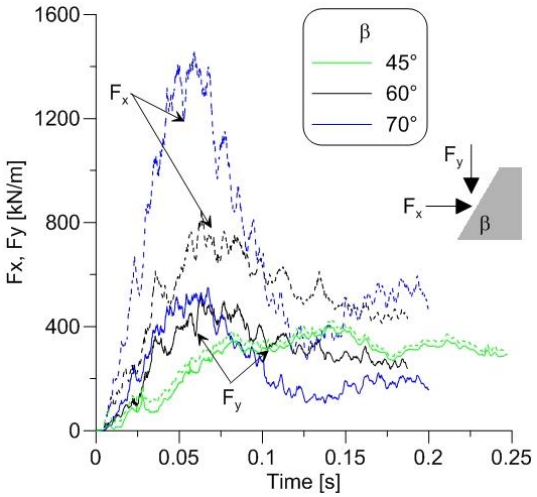

Figure 15 Horizontal force (dashed lines) and vertical force (solid lines) evolution on the structure for different face inclinations (α=90°, v_0=8.8m/s)

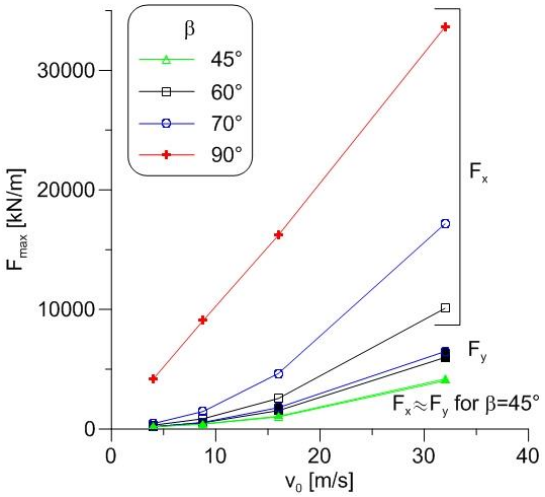

Figure 16 Maximum horizontal and vertical force for different face inclinations and impact velocity (α=90°)

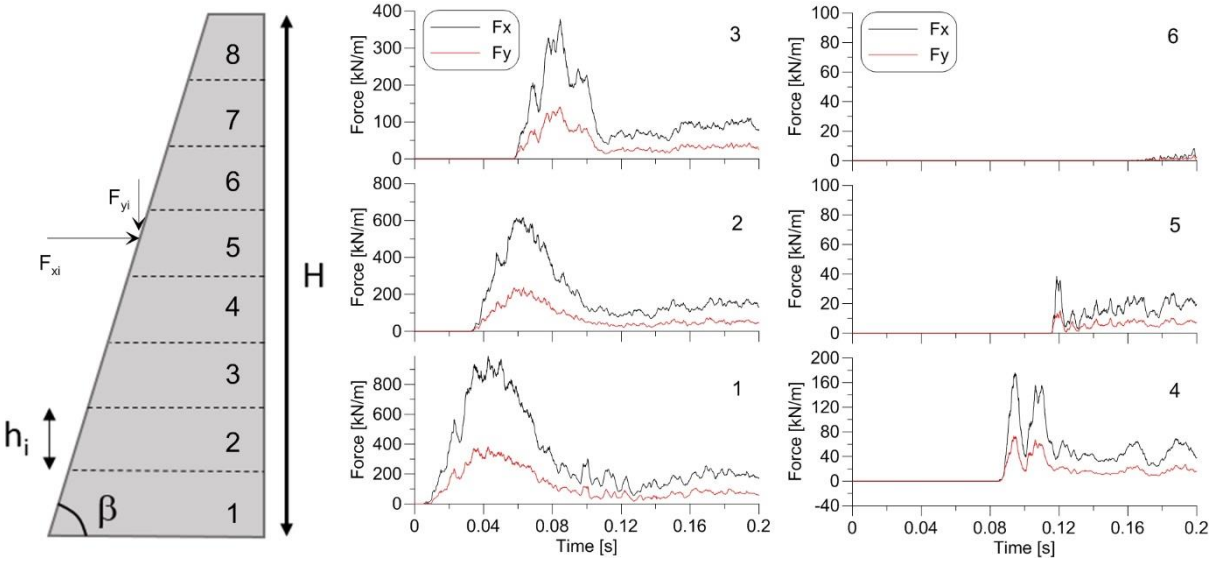

Figure 17 Evolution of impact force applied on each strip in which the dam can be divided (α=90°, β=70°, v_0=8.8m/s)

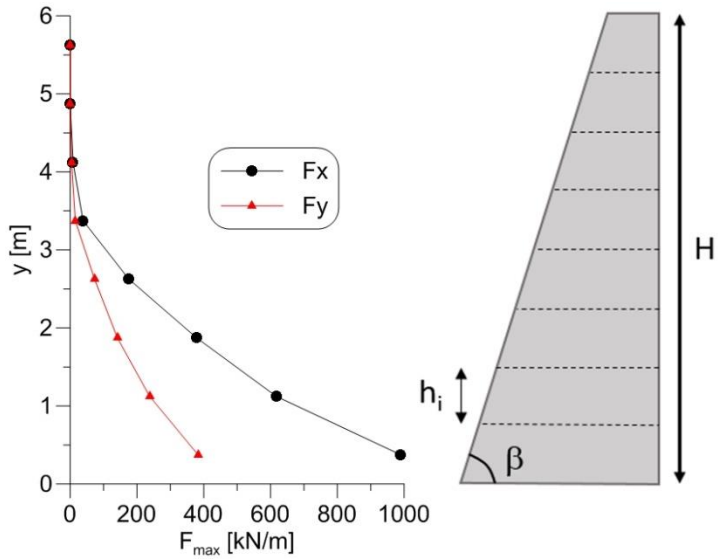

Figure 18 Horizontal and vertical maximum impact force for each strip (α=90°, β=70°, v_0=8.8m/s).

4.4 Effect of wall roughness

Real structures present a rough surface, thus a frictional contact at the soil-structure interface must be taken into account. This is important because the frictional force along the slanted face of the wall increases the horizontal component and reduces the vertical component of the impact force, thus reducing the safety factors for sliding and toppling. We consider a friction coefficient μ between 0 (perfectly smooth surface) and 0.64=*tan(φ)* (very rough surface).
For each time instant, the components of the vertical and horizontal force can be transformed in a normal (F_n) and tangential (F_t) component with the following geometric relationships:

$$F_n = F_x \sin\beta + F_y \cos\beta$$
$$F_t = F_x \cos\beta - F_y \sin\beta$$

Since F_n and F_t are a combination of F_x and F_y, the peak of these components does not occur at the same time instant. Figure 19 shows the evolution of the impact force components for different values of the friction coefficient in the case β=70°. Increasing μ, F_t increases because of friction, thus the vertical component decreases. This has a negative effect on the global stability of the dam and should not be neglected when analysing the sliding ultimate limit state.
The maximum value obtained for each component in the first 0.2s of impact for different values of the friction coefficient is shown in Figure 20, where it can be noted that F_t increases more than linearly with μ, while F_n does not change significantly for this considered value of β.

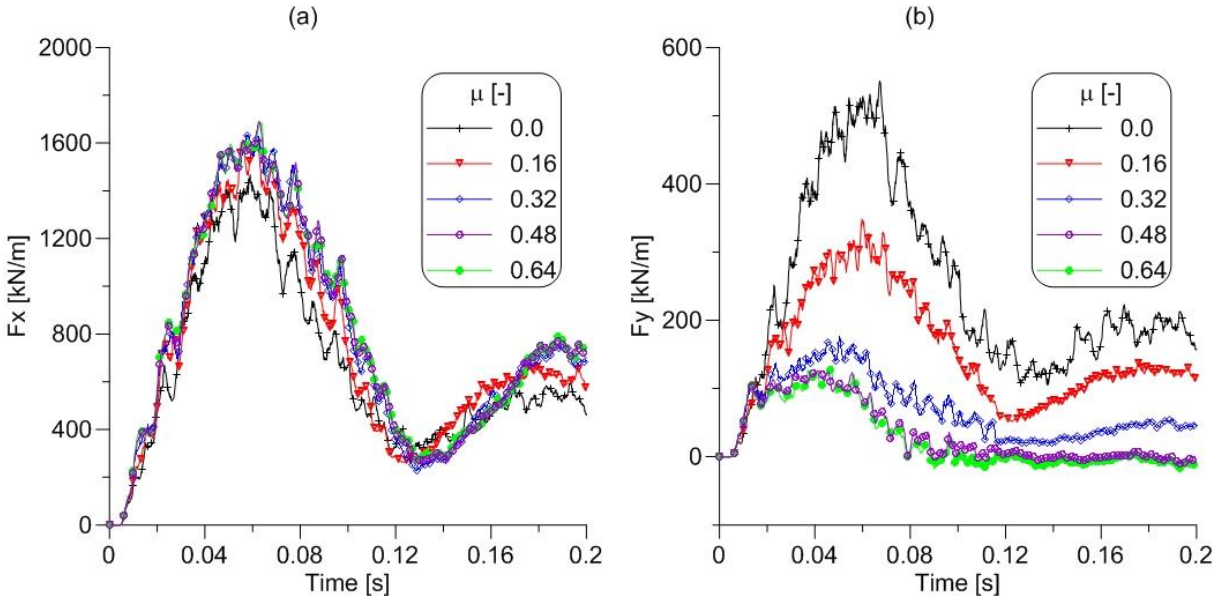

Figure 19 Horizontal (a) and vertical (b) force for different value of the friction coefficient (α=90°, β=70°, v_0=8.8m/s).

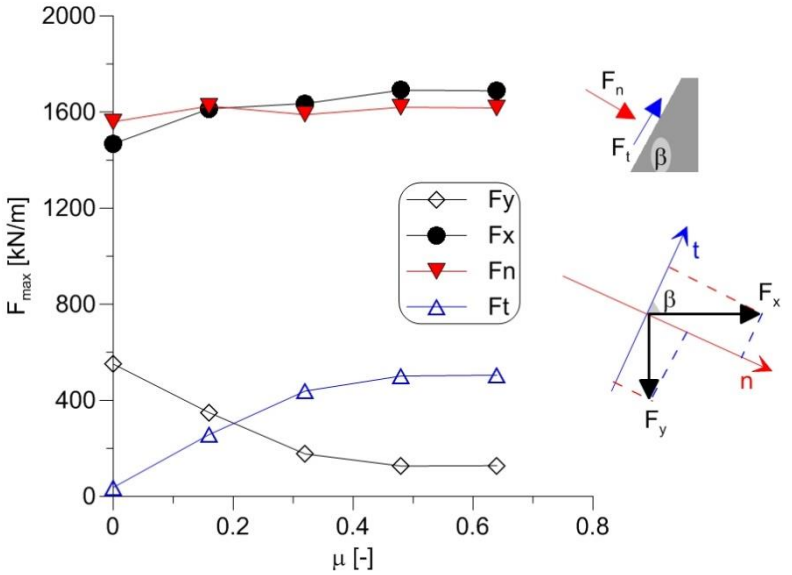

Figure 20 Maximum value of different force components as function of friction coefficient (α=90°, β=70°, v_0=8.8m/s).

4.5 Stresses on an elastoplastic dam

In this Section we remove the hypothesis of rigid structure in order to evaluate the capability of the method to simulate the deformations of the barrier and its possible failure. We consider a dam with α=45°; its constitutive behaviour is modelled with the Mohr-Coulomb criterion with the reference parameters listed in Table 3.

Fix boundary conditions are applied at the base of the dam. No contact algorithm is applied in this set of simulations, due to numerical difficulties in the detection of contact surface in case of large deformations of the structure. This issue will be addressed in the near future.

In Section 4.3 we observed that a low inclination of the barrier face gives lower forces compared to a vertical face and these forces increase more than linearly with the velocity (Figure 16).

Considering v_0=8.8m/s, the granular flow induces an increase of the deviatoric stress at the upstream toe of the dam, but the deformations of the structures are limited (Figure 21).
Increasing the impact velocity to 32m/s, the deviatoric stress on the structure increases significantly, exceeding the material resistance. The dam suffers large deformations and the flow overtop the structure (Figure 22).
Parametric analyses can possibly be performed with *Anura3D* to evaluate the response of the structure for different material parameters or considering different geometries of the dam.

Table 3 Material parameters of the dam

Parameter	**Symbol**	**Value**
Solid density [kg/m^3]	ρ_s	2650
Porosity [-]	n	0.45
Friction angle [°]	φ	37
Dilatancy angle [°]	ψ	5
Cohesion [kPa]	c	20
Young modulus [kPa]	E	60000
Poisson ratio [-]	ν	0.2

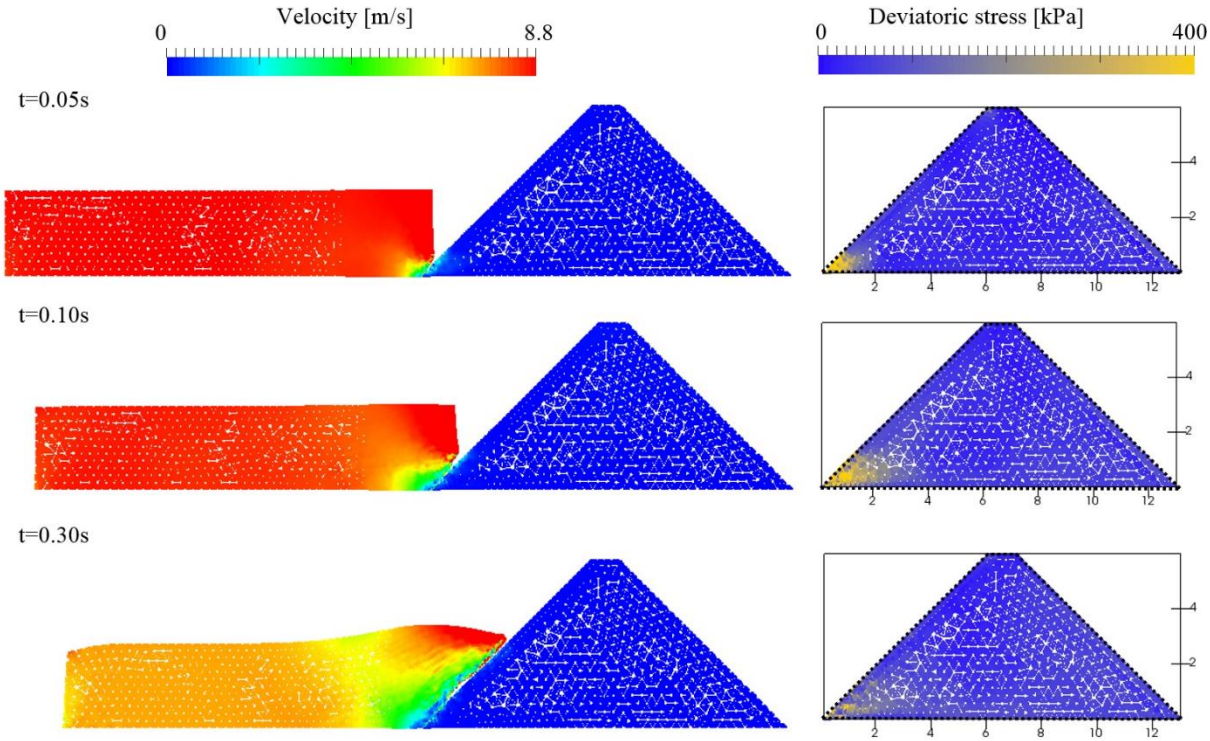

Figure 21 Velocity of the MP (left) and deviatoric stress of the dam (right) at different time instants (α=90°, β=45°, v_0=8.8m/s).

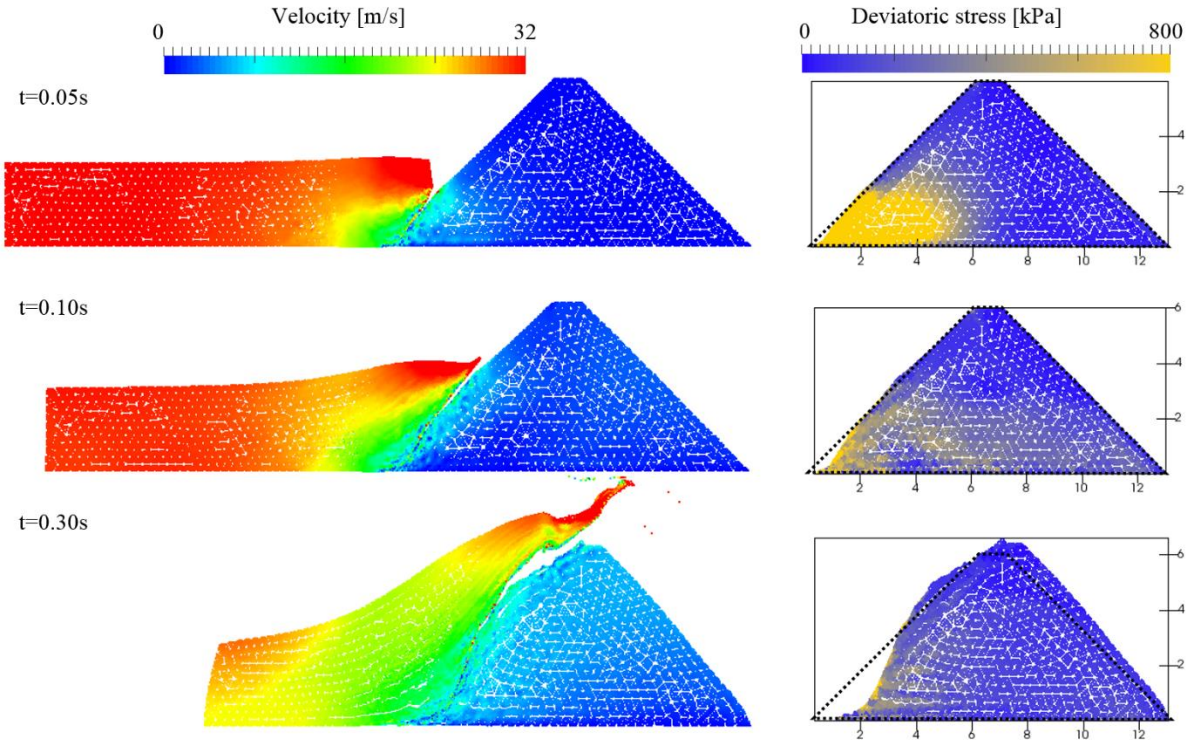

Figure 22 Velocity of the MP (left) and deviatoric stress of the dam (right) at different time instants (α=90°, β=45°, v_0=32m/s).

5 Conclusions and future developments

This papers shows that the MPM can be a valuable tool for an efficient design of protection structures against flow-like landslides. The 3D-implementation allows to consider different shapes of the structures as well as different configurations of the flows.

The paper shows that the method can be applied for the estimate of the run-up on terminal barriers, the obtained results are in good agreement with experimental evidences.

Different geometries of the structure can be easily investigated. In particular, this paper shows the impact on a rigid slanted structure and the effect of the face inclination and roughness on the impact forces. This is particularly important for the global and internal stability of these structures, for which a comprehensive scientific literature of their design under dynamic loading is still missing.

Preliminary analyses have been performed considering the deformability and the shear resistance of the dam, showing that the method can be also applied to investigate the failure modes of the structure. However, further developments of the method are necessary to improve the contact algorithm in case of large deformations of the structure.

Future developments of the research will investigate the internal stability of these barrier and we will consider flexible and permeable structures. A more advanced modelling of the granular flow is also included in our research plan; in particular, more complex constitutive modelling will be implemented and the solid-water interactions will be included.

References

Abe K, Soga K, Bandara S (2013) Material Point Method for Coupled Hydromechanical Problems. J Geotech Geoenvironmental Eng 140:1–16. doi: 10.1061/(ASCE)GT.1943-5606.0001011.

Al-Kafaji IKJ (2013) Formulation of a Dynamic Material Point Method (MPM) for Geomechanical Problems. Ph.D. thesis, University of Struttgart, Germay

Alonso EE, Zabala F (2011) Progressive failure of Aznalcóllar dam using the material point method. Géotechnique 61:795–808. doi: 10.1680/geot.9.P.134

Andersen S, Andersen L (2010) Modelling of landslides with the material-point method. Comput Geosci 14:137–147. doi: 10.1007/s10596-009-9137-y

Bandara S, Soga K (2015) Coupling of soil deformation and pore fluid flow using material point method. Comput Geotech 63:199–214. doi: 10.1016/j.compgeo.2014.09.009

Bardenhagen SG, Guilkey JE, Roessig KM, et al (2001) An improved contact algorithm for the material point method and application to stress propagation in granular material. C - Comput Model Eng Sci 2:509–522.

Berg R, Christopher B, Samtani N (2009) Design and construction of mechanically stabilized earth walls and reinforced soil slopes–Volume I. Fed High W Adm. doi: FHWA-NHI-10-024 & FHWA-NHI-10-025

Beuth L, Vermeer PA (2013) Large deformation analysis of cone penetration testing in undrained clay. In: Hicks M, Dijkstra J, LloretCabot M (eds) Installation Effects in Geotechnical Engineering. Taylor & Francis Group, London, Rotterdam, the Netherlands, pp 1–7

Bolognin M, Martinelli M, Bakker KJ, Jonkman SN (2017) Validation of material point method for soil fluidisation analysis. In: 1st International Conference on the Material Point Method, MPM 2017.

Bui H, Fukagawa R (2013) An improved SPH method for saturated soils and its application to investigate the mechanisms of embankment failure: Case of hydrostatic pore-water pressure. Int Numer Anal Methods Geomech 37:31–50. doi: 10.1002/nag

Calvetti F, di Prisco C, Vairaktaris E (2016) DEM assessment of impact forces of dry granular masses on rigid barriers. Acta Geotech. doi: 10.1007/s11440-016-0434-z

Ceccato F (2016) Study of flow landslide impact forces on protection structures with the Material Point Method. In: Landslides and Engineered Slopes. Experience, Theory and Practice Proceedings of the 12th International Symposium on Landslides. pp 615–620

Ceccato F (2017) Run-up of granular avalanches on protective barriers : a numerical study with the Material Point Method. In: 15th IACMAG. Wuhan, Cina,

Ceccato F, Beuth L, Simonini P (2017) Adhesive contact algorithm for MPM and its application to the simulation of cone penetration in clay. In: MPM conference. Delft, The Netherlands, pp 1–7

Ceccato F, Beuth L, Vermeer PA, Simonini P (2015) Two-phase Material Point Method applied to cone penetration for different drainage conditions. In: Geomechanics from Micro to Macro - Proceedings of the TC105 ISSMGE International Symposium on Geomechanics from Micro to Macro. Cambridge, pp 965–970

Ceccato F, Beuth L, Vermeer PA, Simonini P (2016) Two-phase Material Point Method applied to the study of cone penetration. Comput Geotech 80:440–452. doi: 10.1016/j.compgeo.2016.03.003

Ceccato F, Simonini P (2016) Numerical study of partially drained penetration and pore pressure dissipation in piezocone test. Acta Geotech 12:195–209. doi: 10.1007/s11440-016-0448-6

Detournay C, Dzik E (2006) Nodal Mixed Discretization for tetrahedral elements. In: Proceedings of the 4th International FLAC Symposium on Numerical Modeling in Geomechanics. Madrid,

Fern EJ, de Lange DA, Zwanenburg C, et al (2016) Experimental and Numerical investigations of dyke failures involving soft materials. Eng Geol. doi: 10.1016/j.enggeo.2016.07.006

Harbitz CB, Domaas U, Engen A (2000) Design of snow avalanche deflecting dams. In: Internationale Symposion INTERPRAEVENT 2000 -- Villach, Österreich, Tagungspublikation. pp 383–396

Idelsohn SR, Oñate E, Pin F Del, Calvo N (2006) Fluid–structure interaction using the particle finite element method. Comput Methods Appl Mech Eng 195:2100–2123. doi: 10.1016/j.cma.2005.02.026

Ishikawa N, Inoue R, Hayashi K, et al (2008) Experimental Approach on measurement of impulsive fluid force using debris flow model. Conf Proc interpraevent 1:343–354.

Iverson RM (1997) The physics of debris flows. Rev Geophys 35:245. doi: 10.1029/97RG00426

Jassim I, Stolle D, Vermeer P (2013) Two-phase dynamic analysis by material point method. Int J Numer Anal Methods Geomech Anal methods Geomech 37:2502–2522. doi: 10.1002/nag

Leonardi A, Cabrera M, Wittel FK, et al (2015) Granular front formation in free-surface flow of concentrated suspensions. Phys Rev E 52204:1–10. doi: 10.1103/PhysRevE.92.052204

Leonardi A, Wittel FK, Mendoza M, Herrmann HJ (2014) Coupled DEM-LBM method for the free-surface simulation of heterogeneous suspensions. Comput Part Mech 1:3–13. doi: 10.1007/s40571-014-0001-z

Mancarella D, Hungr O (2010) Analysis of run-up of granular avalanches against steep, adverse slopes and protective barriers. Can Geotech J 47:827–841. doi: 10.1139/T09-143

Martinelli M, Rohe A (2015) Modelling fluidisation and sedimentation using material point method. In: 1st Pan-American Congress on Computational Mechanics.

Mast CM, Arduino P, Mackenzie-Helnwein P, Miller GR (2014a) Simulating granular column collapse using the Material Point Method. Acta Geotech 101–116. doi: 10.1007/s11440-014-0309-0

Mast CM, Arduino P, Miller GR, Mackenzie-Helnwein P (2014b) Avalanche and landslide simulation using the material point method: flow dynamics and force interaction with structures. Comput Geosci 817–830. doi: 10.1007/s10596-014-9428-9

Moriguchi S, Borja RI, Yashima A, Sawada K (2009) Estimating the impact force generated by granular flow on a rigid obstruction. Acta Geotech 4:57–71. doi: 10.1007/s11440-009-0084-5

Pastor M, Haddad B, Sorbino G, et al (2009) A depth-integrated, coupled SPH model for flow-like landslides and related phenomena. Int J Numer Anal Methods Geomech 33:143–172. doi: 10.1002/nag.705

Phuong NTV, van Tol AF, Elkadi ASK, Rohe A (2016) Numerical investigation of pile installation effects in sand using material point method. Comput Geotech 73:58–71. doi: 10.1016/j.compgeo.2015.11.012

Prime N, Dufour F, Darve F (2014) Solid-fluid transition modelling in geomaterials and application to a mudflow interacting with an obstacle. Int J Numer Anal Methods Geomech 38:1341–1361. doi: 10.1002/nag.2260

Saingier G, Deboeuf S, Lagrée P-Y (2016) On the front shape of an inertial granular flow down a rough incline. Phys Fluids 28:53302. doi: 10.1063/1.4948401

Savage SB (1998) Analyses of slow high-concentration flows of granular materials. J Fluid Mech 377:1–26. doi: 10.1017/S0022112098002936

Sulsky D, Chen Z, Schreyer HL (1994) A particle method for hystory-dependent materials. Comput Methods Appl Mech Eng 118:179–196.

Yerro A, Alonso EE, Pinyol NM (2015) The material point method for unsaturated soils. Geotechnique 65:201–217.

Authors

Dr. Ing. Francesca Ceccato
University of Padua
Department of Civil, Environmental and Architectural Engineering
Via Ognissanti 39
35129 Padova, Italy
Tel.: +39 (0) 490-8277991
e-mail: francesca.ceccato@dicea.unipd.it

Prof. Paolo Simonini
University of Padua
Department of Civil, Environmental and Architectural Engineering
Via Ognissanti 39
35129 Padova, Italy
e-mail: paolo.simonini@unipd.it